physica status solidi

pss

www.pss-journals.com

reprint

WILEY-VCH

Phys. Status Solidi B **248**, No. 11, 2676–2679 (2011) / **DOI** 10.1002/pssb.201100127

physica status solidi b
www.pss-b.com
basic solid state physics

Coherent transmission in multiterminal molecular conductors

Lyuba Malysheva[1,2] **and Alexander Onipko**[*,2,3]

[1] Bogolyubov Institute for Theoretical Physics, 03680 Kyiv, Ukraine
[2] Laboratory on Quantum Theory in Linköping, Linköping, Sweden
[3] Division of Molecular Physics, Department of Physics, Chemistry and Biology, Linköping University, 581 83 Linköping, Sweden

Received 1 May 2011, revised 14 June 2011, accepted 6 July 2011
Published online 18 August 2011

Keywords coherent transmission, multiterminal devices, molecular wire junctions, Green's function partitioning, quantum resistance

[*] Corresponding author: e-mail aleon@ifm.liu.se, Phone: +46-13-288904, Fax: +46-13-149403

We consider coherent transport in an arbitrary molecular complex functioning as $\mathcal{N}$-terminal conductor. The matrices that enter Datta's trace formula for the transmission function $T(E)$ are represented in terms of free-molecule Green's function matrix elements referring exclusively to molecular atoms perturbed by the lead–molecule interaction. Explicit expressions of transmission function are obtained for a commonly used model of multiterminal molecular devices, where the molecule is coupled with each lead via a single bond. In the particular cases of connection of molecular wires via a single atom and a benzene ring, this gives the analytical expressions of $T(E)$. Physical implications of the derived formulas are briefly discussed.

A considerable research effort is currently undertaken to decrease the size of electronic devices. This explains rapid development of molecular electronics, where molecules are thought as functional units of electronic circuits. The natural small size and exact reproduction of molecular components promises a number of advantages in comparison with conventional electronic devices. The experimental progress of controlling the current through a single molecule is assisted by intensive theoretical modeling of molecular device performance [1, 2].

Most of works in the field have been focused on the source-molecule-drain model. Electron transmission in multiterminal molecular devices remains thus far a poorly explored area. Recent studies of coherent current in three- and four-terminal systems [3–7] (and references therein) are based on Datta's trace formula [8]

$$T_{j'j} = 4\mathrm{Tr}\left[\mathrm{Im}\boldsymbol{\Sigma}_{j'}\,\boldsymbol{G}\,\mathrm{Im}\boldsymbol{\Sigma}_{j}\,\boldsymbol{G}^{*}\right]. \tag{1}$$

It determines the probability that carriers with energy E entering the conductor from perfect semi-infinite lead j (see Fig. 1), are transmitted to lead j'. According to the original reading of Eq. (1), matrix $\boldsymbol{G}$ describes the whole conductor with the account of conductor–lead interaction by means of self-energy $\boldsymbol{\Sigma} = \sum_j \boldsymbol{\Sigma}_j$. Both $\boldsymbol{G}$ and $\boldsymbol{\Sigma}$ have the same dimensionality as the matrix of conductor Hamiltonian $\boldsymbol{H}^{\mathcal{M}}$. Calculations of $\mathcal{N}\times(\mathcal{N}-1)$ probabilities $T_{j'j}$ requires the knowledge of equal number of submatrices $\boldsymbol{G}_{j'\neq j,j}$. The manifold of these can be treated as submatrices $\boldsymbol{\mathcal{G}}_{j'\neq j,j}$ of another matrix $\boldsymbol{\mathcal{G}}$ built up of matrix elements which refer exclusively to conductor binding atoms. Its dimensionality is thus equal to $[\mathbb{N}\times\mathbb{N}]$, $\mathbb{N} = \sum_{j=1}^{\mathcal{N}} \mathrm{N}_j$. Usually, it is much lower than the dimensionality of $\boldsymbol{G}$.

In this communication, we present the derivation of equations for submatrices $\boldsymbol{\mathcal{G}}_{j'\neq j,j}$ in terms of their counterpart submatrices $\boldsymbol{G}^{\mathcal{M}}_{j'\neq j,j}$ describing the isolated conductor and matrices $\boldsymbol{A}_j = \boldsymbol{V}_j\boldsymbol{G}^{(j)}\boldsymbol{V}_j$ describing the conductor–lead interaction. The obtained equations provide an alternative starting point for calculations of transmission probabilities

$$T_{j'j} = 4\mathrm{Tr}\left(\mathrm{Im}\boldsymbol{A}_{j'}\boldsymbol{\mathcal{G}}_{j',j}\,\mathrm{Im}\boldsymbol{A}_{j}\,\boldsymbol{\mathcal{G}}^{*}_{j,j'}\right). \tag{2}$$

It is shown that for a certain class of multiterminal systems, this formula can be advanced to analytical results which are specified for junctions of molecular wires.

1 Green's function partitioning The way we obtain equations for the set of submatrices $\boldsymbol{\mathcal{G}}_{j'\neq j,j}$ is in the spirit of Löwdin's partitioning technique [9, 10]. Let us

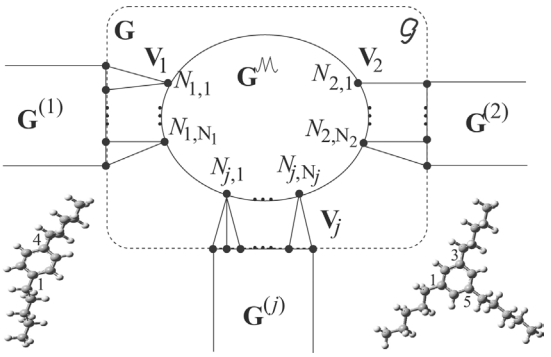

Figure 1 Multiterminal molecular conductor $\mathcal{M}$ coupled to perfect semi-infinite leads via binding atoms $N_{j,l}$, $j=\overline{1,\mathcal{N}}$, $l=\overline{1,\mathrm{N}_j}$. Here, isolated conductor and leads are described by Green's functions $\boldsymbol{G}^{\mathcal{M}}$ and $\boldsymbol{G}^{(j)}$, respectively. Conductor perturbed by the interaction with leads $\boldsymbol{V}=\sum_j \boldsymbol{V}_j$ can be described either by $\boldsymbol{G}=\left(\boldsymbol{I}E-\boldsymbol{H}^{\mathcal{M}}-\sum_j \boldsymbol{\Sigma}_j\right)^{-1}$ as in Ref. [8] or by $\mathcal{G}$ as suggested in present work. Left and right insets show ab initio optimized geometries (BP86/6-31G*) of two- and three-terminal molecular conductors.

denote the manifold of terminal indices $j'\neq j$ as $\{\tilde{j}\}$, so that $\{\tilde{j}\}=1,\ldots,j-1,j+1,\ldots,\mathcal{N}$. Then, the reduced matrix $\boldsymbol{G}^{\mathcal{M}}$ (supposed to be known) can be represented as

$$\boldsymbol{G}^{\mathcal{M}}=\left(\begin{array}{c|ccc} \boldsymbol{G}^{\mathcal{M}}_{j,j} & \boldsymbol{G}^{\mathcal{M}}_{j,1} & \ldots & \boldsymbol{G}^{\mathcal{M}}_{j,\mathcal{N}} \\ \hline \boldsymbol{G}^{\mathcal{M}}_{1,j} & \boldsymbol{G}^{\mathcal{M}}_{1,1} & \ldots & \boldsymbol{G}^{\mathcal{M}}_{1,\mathcal{N}} \\ \ldots & \ldots & \ldots & \ldots \\ \boldsymbol{G}^{\mathcal{M}}_{\mathcal{N},j} & \boldsymbol{G}^{\mathcal{M}}_{\mathcal{N},1} & \ldots & \boldsymbol{G}^{\mathcal{M}}_{\mathcal{N},\mathcal{N}} \end{array}\right) \equiv \left(\begin{array}{cc} \boldsymbol{G}^{\mathcal{M}}_{j,j} & \boldsymbol{G}^{\mathcal{M}}_{j,\{\tilde{j}\}} \\ \boldsymbol{G}^{\mathcal{M}}_{\{\tilde{j}\},j} & \tilde{\boldsymbol{G}}^{\mathcal{M}} \end{array}\right), \tag{3}$$

and similarly, the unknown matrix is $\mathcal{G}=\begin{pmatrix} \mathcal{G}_{j,j} & \mathcal{G}_{j,\{\tilde{j}\}} \\ \mathcal{G}_{\{\tilde{j}\},j} & \tilde{\mathcal{G}} \end{pmatrix}$.

As seen, these matrices are partitioned so that the first and second diagonal members are $[\mathrm{N}_j\times\mathrm{N}_j]$ and $[(\mathbb{N}-\mathrm{N}_j)\times(\mathbb{N}-\mathrm{N}_j)]$ matrices, whereas the off-diagonal members are column and row vectors consisting of $[\mathrm{N}_j\times\mathrm{N}_{j'}]$ matrices. $\mathcal{G}$ and $\boldsymbol{G}^{\mathcal{M}}$ are interrelated by the Dyson equation

$$\mathcal{G}=\boldsymbol{G}^{\mathcal{M}}+\boldsymbol{G}^{\mathcal{M}}\boldsymbol{A}\mathcal{G}, \tag{4}$$

where $\boldsymbol{A}=\begin{pmatrix} \boldsymbol{A}_j & 0 \\ 0 & \tilde{\boldsymbol{A}} \end{pmatrix}$ and $\tilde{\boldsymbol{A}}=\begin{pmatrix} \boldsymbol{A}_1 & \ldots & 0 \\ & \boldsymbol{A}_{j'\neq j} & \\ 0 & \ldots & \boldsymbol{A}_{\mathcal{N}} \end{pmatrix}$.

Solving two equations for the first column members of matrix $\mathcal{G}$, we obtain

$$\left[\boldsymbol{I}-\tilde{\boldsymbol{G}}^{\mathcal{M}}\tilde{\boldsymbol{A}}-\boldsymbol{G}^{\mathcal{M}}_{\{\tilde{j}\},j}\boldsymbol{A}_j\left(\boldsymbol{I}-\boldsymbol{G}^{\mathcal{M}}_{j,j}\boldsymbol{A}_j\right)^{-1}\boldsymbol{G}^{\mathcal{M}}_{j,\{\tilde{j}\}}\tilde{\boldsymbol{A}}\right]\mathcal{G}_{\{\tilde{j}\},j} = \boldsymbol{G}^{\mathcal{M}}_{\{\tilde{j}\},j}\left(\boldsymbol{I}-\boldsymbol{A}_j\boldsymbol{G}^{\mathcal{M}}_{j,j}\right)^{-1}. \tag{5}$$

Equation (5) determines components of column vector $\mathcal{G}_{\{\tilde{j}\},j}$ which enter the transmission formula (2). One can go the other way round and obtain an analogous equation for row vector $\mathcal{G}_{j,\{\tilde{j}\}}$. It can be proved that $\mathcal{G}_{j',j}=\mathcal{G}^{T}_{j,j'}$. Hence, the choice of fixed terminal index as well as the use of either above equation or its analog for the row vector is just the matter of convenience.

In most of studies, the molecular conductor is supposed to be coupled to each lead via a single atom (in Fig. 1, $N_{j,l}\to N_j$). Then, all entries in matrices $\boldsymbol{G}^{\mathcal{M}}$ and $\boldsymbol{A}$ are scalars. For such models, Eq. (5) can be simplified to [11]

$$\sum_{j''\neq j} M_{j',j''}\mathcal{G}_{j'',j}=G^{\mathcal{M}}_{j',j}, \tag{6}$$

where $M_{j',j''}=\left(1-A_jG^{\mathcal{M}}_{N_j,N_j}\right)\left(\delta_{j',j''}-A_{j''}G^{\mathcal{M}}_{N_{j'},N_{j''}}\right)-A_jA_{j''}G^{\mathcal{M}}_{N_j,N_{j'}}G^{\mathcal{M}}_{N_{j''},N_j}$.

In general, solving Eq. (6) is a computational problem. However, an exception is presented by symmetric molecular systems, where matrix elements $G^{\mathcal{M}}_{N_j,N_{j'\neq j}}=G^{\mathcal{M}}_{nd}$ and $G^{\mathcal{M}}_{N_j,N_j}=G^{\mathcal{M}}_{d}$ do not depend on j. This model, which is relevant to junctions of molecular wires exemplified in Fig. 1, admits obtaining an explicit solution without any restriction on the coupling functions A_j. It reads

$$\mathcal{G}_{j',j}=\frac{G^{\mathcal{M}}_{nd}}{Q_jQ_{j'}\left[1-G^{\mathcal{M}}_{nd}\sum_{j''=1}^{\mathcal{N}}A_{j''}Q^{-1}_{j''}\right]}, \tag{7}$$

where $Q_j\equiv 1-A_j\left(G^{\mathcal{M}}_{d}-G^{\mathcal{M}}_{nd}\right)$. Some of applications of this equation are discussed next.

2 Molecular Green's function for symmetric junctions of molecular wires Junctions of molecular wires can be thought as a set of chain-like molecules coupled to a "connector". In Fig. 1, the connector is represented by benzene ring. It can also be an annulene ring (like cyclooctadecanonaene) or more complex molecule. The simplest connector is realized by a carbon atom or heteroatom.

The Green's function of molecular wire junction can be expressed in terms of wire Green's functions G^{w_j} and connector Green's function G^{c} by solving the Dyson equation

$$G^{\mathcal{M}}_{n,n'}=G^{0}_{n,n'}-\sum_{n'',n'''}G^{0}_{n,n''}V_{n'',n'''}G^{\mathcal{M}}_{n''',n'}, \tag{8}$$

where indices of matrix elements run over molecular atoms; $G^{0}_{n,n'}=G^{w_j}_{n,n'}$, if n, n' belong to wire j, or $G^{0}_{n,n'}=G^{c}_{n,n'}$, if n, n' belong to the connector; otherwise $G^{0}_{n,n'}=0$. Labeling the binding atoms within wire/connector by $1j$ from the side of wire and $\{x\}$ from the side of connector (in Fig. 1, x-atoms are 1,4 and 1,3,5), the wire–connector interaction can be represented as $V_{n,n'}=\sum_j\mathcal{V}_j(\delta_{n,\{x\}}\delta_{n',1j}+\delta_{n',\{x\}}\delta_{n,1j})$, where $\mathcal{V}_j$ denotes the wire-connector hopping integral.

For symmetric connectors, all diagonal and off-diagonal matrix elements which appear in Eq. (8) are equal, $G^{c}_{x,x}=G^{c}_{d}$, $G_{x,x'}=G^{c}_{nd}$. Then, the solution for $G^{\mathcal{M}}_{N_j,N_j}$ and

$G^{\mathcal{M}}_{N_j,N_{j'}}$ takes the form

$$G^{\mathcal{M}}_{N_j,N_{j'}} = \delta_{j,j'}\left[G^{w_j}_{N_j,N_j} + \left(G^c_d - G^c_{nd}\right)\left(\mathcal{V}_j G^{w_j}_{1j,N_j}\right)^2 \mathcal{D}_j^{-1}\right] + G^c_{nd}\frac{\mathcal{V}_j\mathcal{V}_{j'}G^{w_j}_{1j,N_j}G^{w_{j'}}_{1j',N_{j'}}}{\mathcal{D}_j\mathcal{D}_{j'}\left(1 - G^c_{nd}\sum\limits_{j''=1}^{\mathcal{N}}\mathcal{V}^2_{j''}G^{w_{j''}}_{1j'',1j''}\mathcal{D}^{-1}_{j''}\right)}, \quad (9)$$

where $\mathcal{D}_j = 1-\left(G^c_d - G^c_{nd}\right)\mathcal{V}^2_j G^{w_j}_{1j,1j}$. For junctions of identical wires, $\mathcal{D} = 1-\left(G^c_d - G^c_{nd}\right)\mathcal{V}^2 G^w_{1,1}$, and

$$G^{\mathcal{M}}_{nd} = G^c_{nd}\left(\mathcal{V}G^w_{1,N}\right)^2\left(\mathcal{D} - \mathcal{N}\mathcal{V}^2 G^c_{nd}G^w_{1,1}\right)^{-1}\mathcal{D}^{-1},$$
$$G^{\mathcal{M}}_{d} = G^{\mathcal{M}}_{nd} + G^w_{N,N} + \left(G^c_d - G^c_{nd}\right)\left(\mathcal{V}G^w_{1,N}\right)^2\mathcal{D}^{-1}. \quad (10)$$

Green's functions of many chain-like molecules (linear oligomers) have an analytical expression in the wave-vector representation. In particular, for the commonly used model of N-site tight-binding chain, the required matrix elements are [12]

$$\begin{Bmatrix} G^w_{1,1} \\ G^w_{1,N} \end{Bmatrix} = -\frac{1}{\beta\sin\left[(N+1)k\right]}\begin{Bmatrix} \sin(Nk) \\ \sin k \end{Bmatrix}, \quad (11)$$

where k is related to energy as $E = -2\beta\cos k$.

For the benzene connector, the required matrix elements are given by $G^c_d = E(E^2-3\beta^2)/D_c$, $G^c_{nd} = E\beta^2/D_c$ (binding sites 1,3), and $G^c_{nd} = -2\beta^3/D_c$ (binding sites 1,4), $D_c = (E^2-\beta^2)(E^2-4\beta^2)$. Zero site energy and the same hopping integral β are assumed for wires and benzene connector. For a single-atom connector with the site energy ε, $G^c_d = G^c_{nd} = (E-\varepsilon)^{-1}$. Taken together with Eqs. (10) and (11), these expressions complete the definition of molecular Green's function for symmetric junctions of identical wires.

Note that the above derivations assume the wave-like motion of charge carriers. The dephasing effects are thus disregarded but they can be included into the presented scheme either by a phenomenological re-definition of self-energy [13] or by adding an extra term of "non-coherent" transmission in Eq. (1) [14].

3 Transmission through $\mathcal{N}$-wire junctions

Consider first the transmission through junctions formed by single-atom connectors. Let all but one coupling functions be equal, $A_{j\neq 1}=A$. The chain of substitutions $G^{\mathcal{M}} \to \mathcal{G}_{j,1} \to T_{j1} \equiv T_{\mathcal{N}}$ and long but straightforward algebra lead to the following expression

$$T_{\mathcal{N}} = 4A^{\mathcal{I}}A^{\mathcal{I}}_1\sin^4 k\Big|\{\sin[(N+1)k] + A_1\sin(Nk)\}\cdot \times\left[\mathcal{N}\mathcal{F}_{N-1} + (E-\varepsilon)\mathcal{F}_N\mathcal{V}^{-2}\right] + (A-A_1)\sin^2 k\Big|^{-2}, \quad (12)$$

where $\mathcal{F}_N = \sin[(N+1)k] + A\sin(Nk)$, and all energy quantities are in units of β without change in notations.

To expose the transmission dependence on the wire–lead coupling strength and number of wires, it is instructive to use the WBL approximation $A = -i\alpha$, $A_1 = -i\alpha_1$ [15]. The physical meaning of coupling parameters can be understood from its definition for one-dimensional leads, $\alpha_j = V_j^2/(\beta\beta'_j)$, where V_j and β'_j are, respectively, the wire–lead and in-lead hopping integrals. The analysis of Eq. (12) shows that the transmission is controlled by combined coupling parameters $\alpha\alpha_1 \equiv \exp(2\gamma)$ and $\alpha/\alpha_1 \equiv \exp(2\nu)$. The former can be regarded as a characteristic of coupling strength, the latter characterizes the coupling asymmetry. In terms of these quantities and under restrictions $N \gtrsim 10$, $E \lesssim 0.5$, $\mathcal{V} = 1$, and $\varepsilon = 0$, the WBL version of Eq. (12) is accurately reproduced by

$$T_{\mathcal{N}} \approx \frac{4}{\mathcal{N}^2}\left\{\sin^2(2Nk)\cosh^2\gamma + \left[2\sin^2(Nk)\cosh\nu - e^{\nu} + 2\mathcal{N}^{-1}\sinh\nu\right]^2\right\}^{-1}, \quad (13)$$

and following from it for $\alpha = \alpha_1$,

$$T_{\mathcal{N}} \approx \frac{4}{\mathcal{N}^2}\left[1 + \sinh^2\gamma\,\sin^2(2Nk)\right]^{-1} = \frac{4}{\mathcal{N}^2}T_2, \quad (14)$$

and for $\mathcal{N} = 2$,

$$T_2 \approx \left[\cosh^2\nu + (\sinh^2\gamma - \sinh^2\nu)\,\sin^2(2Nk)\right]^{-1}. \quad (15)$$

Factor $1/\mathcal{N}^2$ in Eq. (14) is worth noting. For the given model of two-wire junction (that is for a $(2N+1)$-long wire connected to the source and drain), the current driven by constant potential difference U can be represented in the form of Ohm's law $I_2 = U/R_q$, where the quantum resistance is defined as $R_q^{-1} = (2e/h)\int_{-\infty}^{\infty}T_2(E)f(E)\mathrm{d}E/U$ with an appropriate weight factor f [8]. In classic description, the current through two conventional resistors R connected in series equals $U/2R$. If instead of one N-long wire (or resistor R), the junction is continued by $\mathcal{N}-1$ wires (resistors) (and each is connected to its drain at the same potential), the drain current $I_{\mathcal{N}} = 4U/\mathcal{N}^2R_q$, according to Eq. (14), but it equals $U/\mathcal{N}R$, according to the Ohm law and conservation of current. This comparison shows that for junctions of quantum and conventional wires, the drain current is governed by qualitatively different dependencies on $\mathcal{N}$; specifically, by $\sim 1/\mathcal{N}^2$ and $\sim 1/\mathcal{N}$. However, for the number of wires from three to five, both descriptions of current branching give quantitatively close results in terms of respective resistances.

Some peculiar features of the transmission dependence on coupling parameters are illustrated in Fig. 2. For symmetric coupling, $\alpha_1 = \alpha$ (or $\nu = 0$), maximal transmission probability $T^{\max}_{\mathcal{N}} = 4/\mathcal{N}^2$ is independent of coupling strength. But it can be larger or smaller than this if $\alpha_1 \neq \alpha$. The coupling asymmetry also alters the overall spectrum shape. In both cases of symmetric and asymmetric coupling, an increase of γ results in a counterintuitive effect. The left panel in Fig. 2 (symmetric coupling) shows that the resonance structure becomes more pronounced (in contrast to often stated

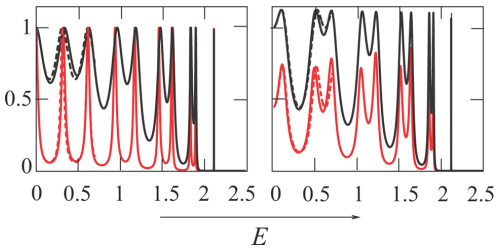

Figure 2 (online color at: www.pss-b.com) Normalized transmission spectrum $T_{\mathcal{N}}\mathcal{N}^2/4$ ($\mathcal{N}=3$, $N=10$) calculated in the WBL approximation: (12) solid lines, (13) dashed lines. Panel to the left represents symmetric coupling with $\alpha=2$ (in black) and $\alpha=8$ (in red). Panel to the right represents asymmetric coupling with $\alpha=1/2$, $\alpha_1=2$ (in black) and $\alpha=1/2$, $\alpha_1=8$ (in red).

broadening of transmission resonances). In the right panel (asymmetric coupling), we see instead that the transmission is suppressed by increase of γ (at the expense of α_1 larger value).

The extremely sharp resonance which is seen on the right hand side of presented spectra attracts attention. It originates from the bound state which is characteristic for junctions with a single-atom connector [11]. As shown below, the transmission spectrum of benzene based junctions possesses similar feature.

In the interests of simplicity, we restrict ourselves by the consideration of identical coupling in which case Eqs. (2) and (7) can be combined into

$$T_{\mathcal{N}} = 4(A^{\mathcal{I}})^2\left(G^{\mathcal{M}}_{nd}\right)^2\left|1-A(G^{\mathcal{M}}_{d}-G^{\mathcal{M}}_{nd})\right|^{-2} \times\left|1-A\left[G^{\mathcal{M}}_{d}+(\mathcal{N}-1)G^{\mathcal{M}}_{nd}\right]\right|^{-2}. \tag{16}$$

The transmission spectra described by the above equation are represented in Fig. 3. They show the presence of delta-like peaks which have not appeared in previous studies of this type of junctions. The bound state nature of these resonances is proven by their spectral position.

Indeed, according to Eq. (10), the junction spectrum is determined by equations $\mathcal{D}=0$ and $\mathcal{D}_{\mathcal{N}}\equiv\mathcal{D}-\mathcal{N}\mathcal{V}^2G^{c}_{nd}G^{w}_{1,1}=0$. We have estimated solutions to these equations, taking into account that for $E>2$, $k=\pi+i\delta$ and hence, we have $G^{w}_{1,N}\approx(-1)^{N+1}e^{-N\delta}$, $G^{w}_{1,1}\approx e^{-\delta}$, if $N\gtrsim 5$. Exploiting these

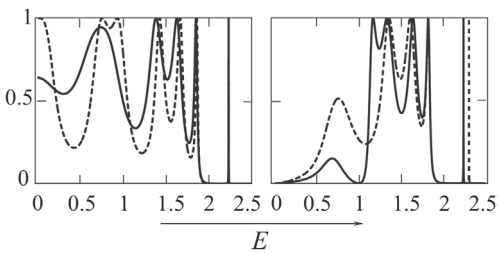

Figure 3 Normalized transmission spectrum $T_{\mathcal{N}}\mathcal{N}^2/4$ ($N=5$, $\mathcal{V}=1$) calculated from Eq. (16) in the WBL approximation. Panel to the left represents two-wire junction, connection 1,4; $\alpha=1$ (solid line) and $\alpha=1/2$ (dashed line). Panel to the right represents two-wire junction, connection 1,3 (solid line) and three-wire junction, connection 1,3,5 (dashed line); $\alpha=1$.

expressions and (as G^{c}_{nd}) benzene Green's function in the secular equations, it is easy to prove the following. For two-terminal junctions with wires coupled to atoms 1,4, it is equation $\mathcal{D}=0$ or equivalently, $2\sinh\delta=e^{-\delta}$ that has the root $e^{\delta}=(1+\sqrt{5})/2$. It gives the bound state energy $E=2.236$, in perfect agreement with the position of out-of-band peak in Fig. 3 (left). For two-terminal junction with wires coupled to atoms 1,3 and for three-terminal junctions with wires coupled to atoms 1,3,5, only equation $\mathcal{D}_{\mathcal{N}}=0$ or $2e^{3\delta}\sinh^2\delta/\cosh\delta=\mathcal{V}^2\mathcal{N}$ has appropriate roots. As an example, assuming that $\mathcal{V}=1$ we obtain $E=2.244$ for $\mathcal{N}=2$ and $E=2.309$ for $\mathcal{N}=3$, also in a very good agreement with the position of corresponding resonances in Fig. 3 (right).

In conclusion, the exact explicit expression of transmission coefficient is derived for symmetric junctions of molecular wires. It describes the dependence of coherent transport on the wire–lead coupling (specified in terms of Hamiltonian parameters) and the number of wires $\mathcal{N}$. The transmission spectrum is shown to be scaled by factor $4/\mathcal{N}^2$ that determines the maximal probability of transmission through junctions coupled to external leads identically. The coupling asymmetry can increase or decrease this value. It is also shown that the bound states, which appear due to wire coupling via a single atom or molecular connector, give rise to resonances above and below the wire band edges. These inherent properties of multiterminal molecular conductors are to be studied further in the context of specific experimental realizations.

Acknowledgements This work was partly supported by Visby program of the Swedish Institute (SI) and Special Program of Division of Physics and Astronomy of NASU.

References

[1] A. Nitzan and M. A. Ratner, Science **300**, 1384 (2003).
[2] F. Chen and N. J. Tao, Acc. Chem. Res. **42**, 429 (2009).
[3] L. Wang, K. Tagami, and M. Tsukada, Jpn. J. Appl. Phys. **43**, 2779 (2004).
[4] D. M. Cardamone, C. A. Stafford, and S. Mazumdar, Nano Lett. **6**, 2422 (2006).
[5] P. Dutta, S. K. Maiti, and S. N. Karmakar, Org. Electron. **11**, 1120 (2010).
[6] S. K. Maiti, Solid State Commun. **150**, 1269 (2010).
[7] K. K. Saha, W. Lu, J. Bernholc, and V. Meunier, Phys. Rev. B **81**, 125420 (2010).
[8] S. Datta, Electronic Transport in Mesoscopic Systems (Cambridge University Press, Cambridge, 1995).
[9] P. O. Löwdin, J. Math. Phys. 969, (1962).
[10] A. Onipko and L. Malysheva, in: Handbook on Nano- and Molecular Electronics (CRC Press, 2007), chap. 23.
[11] L. Malysheva and A. Onipko, submitted.
[12] K. Lakatos-Lindenberg, R. P. Hemenger, and P. M. Pearlstein, J. Chem. Phys. **56**, 4852 (1972).
[13] R. Golizadeh-Mojarad and S. Datta, Phys. Rev. B **75**, 081301(R) (2007).
[14] M. Dey, S. K. Maiti, and S. N. Karmakar, Org. Electron. **12**, 1017 (2011).
[15] A. Prociuk, B. Van Kuiken, and B. D. Dunietz, J. Chem. Phys. **125**, 204717 (2006).